

Fig. 1 Chronic GVHD-specific survival in patients with chronic GVHD diagnosed by the NIH consensus criteria. **a** Probability of chronic GVHD-specific survival (cGSS) among patients who developed classic chronic GVHD (solid line) and overlap syndrome (dotted line). **b** Probability of cGSS among patients who developed mild (short dashed line), moderate (long dashed line), and severe chronic GVHD (solid line)

improved grading scales for established cGVHD. A retrospective analysis of data on HLA-identical sibling transplantation reported to the International Bone Marrow Transplant Registry identified five variables independently associated with worse survival of those who developed historic cGVHD: low Karnofsky performance status at cGVHD diagnosis (<80), chronic diarrhea, weight loss, presence of cutaneous manifestation, and lack of oral involvement [15]. The Seattle group also proposed a revised classification for distinguishing limited and extensive cGVHD by the use of 16 clinical criteria [16]. Although these new classifications do not clearly discriminate between cGVHD and delayed onset GVHD with features resembling aGVHD, they have been shown to be at least useful for identifying patients at higher risk of NRM. Future studies are strongly warranted to compare the prognostic values of NIH cGVHD subcategories with those determined by other cGVHD grading system [21].

So far, several groups have reported the prognostic relevance of cGVHD severity graded by the NIH criteria and consistently found the inferior survival of patients with severe cGVHD [20–23], although such association was not observed in one earlier study [19]. While only a few of these studies focused on the significance of

distinction between “overlap syndrome” and “classic cGVHD”, our study revealed a trend toward worse survival in patients with overlap syndrome compared to those with classic GVHD, as was recently reported by Kim et al. [23]. In the present study, patients with overlap syndrome had a significantly shorter median time to the development of cGVHD than patients with classic cGVHD and were more likely to receive corticosteroid treatment for prior aGVHD at the onset of cGVHD. Intriguingly, these observations were very similar to the findings by Arora et al. [22], who reported that most of patients with overlap syndrome had a history of prior aGVHD and a progressive cGVHD onset, although they did not observe worse survival of this subgroup of patients compared to those with classic cGVHD. Given that nearly all patients who developed overlap syndrome had a prior history of aGVHD in our study cohort, NIH overlap syndrome in most instances could be considered as a flare of pre-existing aGVHD, concomitant with development of classic cGVHD. In this context, it is important to note that early flare of cGVHD or early treatment change for exacerbation of cGVHD has been reported to be associated with increased NRM and inferior cGSS [34, 35]. It is also of note that a significantly higher proportion of patients with overlap syndrome had thrombocytopenia less than $100 \times 10^3/\mu\text{L}$ at cGVHD onset in our study. Since the progressive cGVHD onset and the presence of thrombocytopenia were consistently associated with an increased NRM across various studies [16, 36], more effective management of patients with overlap syndrome and thrombocytopenia might be needed.

Duration of systemic immunosuppressive therapy is suggested to be a useful surrogate endpoint to evaluate the response to specific treatment for cGVHD [26]. Although we could not find significant association of NIH cGVHD subtypes with duration of systemic IST, patients who had been given ongoing systemic corticosteroids at the onset of cGVHD were found to receive significantly prolonged systemic IST in multivariable analysis, consistent with the findings of Vigorito et al. [37]. In our study, the duration of systemic IST was also prolonged in patients who had high-risk underlying disease compared with those who had standard-risk disease. If the activity of cGVHD were likely to worsen in the high-risk subgroup of patients, one possible explanation might be the preference of physicians to taper systemic IST faster for patients at higher risk of relapse.

The present study, however, has several limitations; the retrospective study design, small cohort size, recording bias, and heterogeneity of underlying diseases and transplantation procedures might substantially influence the results. In addition, diagnostic cGVHD manifestations of affected organs or sites might have originated from other causes, including drug reactions, infection, and

Table 3 Univariable and multivariable analysis of factors potentially associated with chronic GVHD-specific survival among patients who developed chronic GVHD defined by the National Institutes of Health criteria

Variable	n (%)	Univariable analysis		Multivariable analysis	
		HR (95% CI)	P value	HR (95% CI)	P value
Patient age					
Less than 50 years	51 (53)	1.00		–	
50 years or more	45 (47)	1.40 (0.49–4.05)	0.53	–	
Donor/recipient sex combination					
Other than female/male	69 (72)	1.00		–	
Female/male	27 (28)	1.03 (0.32–3.28)	0.97	–	
Disease status at transplant					
Standard risk	51 (53)	1.00		1.00	
High risk	45 (47)	3.03 (0.95–9.68)	0.061	2.75 (0.86–8.80)	0.088
Donor/recipient HLA compatibility					
Matched	80 (83)	1.00		–	
Mismatched	16 (17)	0.33 (0.04–2.53)	0.29	–	
Conditioning regimen					
Myeloablative intensity	54 (56)	1.00		–	
Reduced intensity	42 (44)	1.04 (0.36–3.00)	0.95	–	
Stem cell source					
Bone marrow	67 (70)	1.00		–	
Peripheral blood	24 (25)	2.07 (0.69–6.19)	0.19	–	
Cord blood	5 (5)	1.63 (0.57–4.68)	0.37	–	
Prior aGVHD					
Grade 0–1	47 (49)	1.00		–	
Grade 2–4	49 (51)	1.16 (0.40–3.37)	0.78	–	
Subcategory of cGVHD					
Classic cGVHD	77 (80)	1.00		–	
Overlap syndrome	19 (20)	2.76 (0.96–7.97)	0.060	–	
Severity of cGVHD at onset					
Mild to moderate	73 (76)	1.00		1.00	
Severe	23 (24)	3.10 (1.09–8.86)	0.034	2.58 (0.90–7.39)	0.077
Platelet count at cGVHD onset					
100 × 10 ³ /μL or more	65 (68)	1.00		1.00	
Less than 100 × 10 ³ /μL	31 (32)	4.19 (1.40–12.5)	0.010	4.05 (1.35–12.1)	0.013
Eosinophil count at cGVHD onset					
Less than 500/μL	68 (71)	1.00		–	
500/μL or more	28 (29)	0.90 (0.28–2.88)	0.86	–	
Systemic corticosteroids at cGVHD onset					
Not received	63 (66)	1.00		–	
Received	33 (34)	1.74 (0.61–4.97)	0.30	–	

CI confidence interval, aGVHD acute graft-versus-host disease, cGVHD chronic graft-versus-host disease

comorbidity before transplantation. Furthermore, genital tract involvement might be underestimated because female patients do not always report about their genital symptoms to physicians.

In conclusion, our present study suggests that both the subcategory and global severity of cGVHD proposed by

NIH consensus criteria have effects on cGSS and the risk of NRM among patients who develop NIH cGVHD. Future prospective studies are warranted to more precisely characterize the clinical significance of the subcategory and severity of cGVHD evaluated by the NIH consensus criteria.

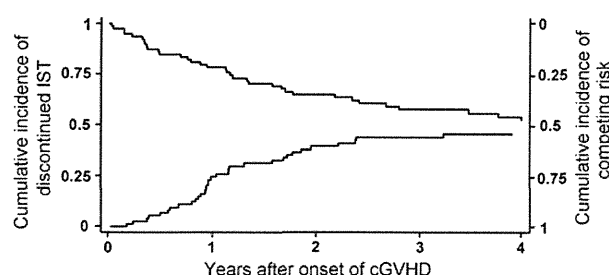


Fig. 2 Cumulative incidence of discontinued systemic immunosuppressive treatment. The *lower curve* shows the cumulative incidence of discontinued systemic immunosuppressive treatment (IST) in the absence of death, recurrent primary disease, or secondary malignancy among 81 patients who developed NIH cGVHD and received systemic IST (*left-hand scale*). The *upper curve* shows the competing risks of death or recurrent/secondary malignancy during systemic IST (*right-hand scale*). At the onset of cGVHD, 69 patients had been already given ongoing systemic IST consisting of calcineurin inhibitors alone ($n = 36$), calcineurin inhibitors plus corticosteroids ($n = 27$), corticosteroids alone ($n = 4$), or corticosteroids plus mycophenolate mofetil ($n = 2$)

Acknowledgments The authors are grateful to Rie Goi and Mika Kobayashi, for their expert data management and secretarial assistance, and all the staff of our transplant team for their dedicated care of the patients and donors.

Conflict of interest The authors have no conflict of interest to declare.

References

- Lee S, Flowers M. Recognizing and managing chronic graft-versus-host disease. *Hematology Am Soc Hematol Educ Program*. 2008;134–41.
- Atkinson K, Horowitz M, Gale R, et al. Risk factors for chronic graft-versus-host disease after HLA-identical sibling bone marrow transplantation. *Blood*. 1990;75:2459–64.
- Higman M, Vogelsang G. Chronic graft versus host disease. *Br J Haematol*. 2004;125:435–54.
- Wagner J, Flowers M, Longton G, Storb R, Schubert M, Sullivan K. The development of chronic graft-versus-host disease: an analysis of screening studies and the impact of corticosteroid use at 100 days after transplantation. *Bone Marrow Transplant*. 1998;22:139–46.
- Przepiorka D, Anderlini P, Saliba R, et al. Chronic graft-versus-host disease after allogeneic blood stem cell transplantation. *Blood*. 2001;98:1695–700.
- Carlens S, Ringdén O, Remberger M, et al. Risk factors for chronic graft-versus-host disease after bone marrow transplantation: a retrospective single centre analysis. *Bone Marrow Transplant*. 1998;22:755–61.
- Cutler C, Giri S, Jeyapalan S, Paniagua D, Viswanathan A, Antin J. Acute and chronic graft-versus-host disease after allogeneic peripheral-blood stem-cell and bone marrow transplantation: a meta-analysis. *J Clin Oncol*. 2001;19:3685–91.
- Mohty M, Kuentz M, Michallet M, et al. Chronic graft-versus-host disease after allogeneic blood stem cell transplantation: long-term results of a randomized study. *Blood*. 2002;100:3128–34.
- Randolph S, Gooley T, Warren E, Appelbaum F, Riddell S. Female donors contribute to a selective graft-versus-leukemia effect in male recipients of HLA-matched, related hematopoietic stem cell transplants. *Blood*. 2004;103:347–52.
- Atsuta Y, Suzuki R, Yamamoto K, et al. Risk and prognostic factors for Japanese patients with chronic graft-versus-host disease after bone marrow transplantation. *Bone Marrow Transplant*. 2006;37:289–96.
- McClune B, Weisdorf D, Pedersen T, et al. Effect of age on outcome of reduced-intensity hematopoietic cell transplantation for older patients with acute myeloid leukemia in first complete remission or with myelodysplastic syndrome. *J Clin Oncol*. 2010;28:1878–87.
- Mielcarek M, Martin P, Leisenring W, et al. Graft-versus-host disease after nonmyeloablative versus conventional hematopoietic stem cell transplantation. *Blood*. 2003;102:756–62.
- Mielcarek M, Burroughs L, Leisenring W, et al. Prognostic relevance of ‘early-onset’ graft-versus-host disease following non-myeloablative haematopoietic cell transplantation. *Br J Haematol*. 2005;129:381–91.
- Shulman H, Sullivan K, Weiden P, et al. Chronic graft-versus-host syndrome in man. A long-term clinicopathologic study of 20 Seattle patients. *Am J Med*. 1980;69:204–17.
- Lee S, Klein J, Barrett A, et al. Severity of chronic graft-versus-host disease: association with treatment-related mortality and relapse. *Blood*. 2002;100:406–14.
- Lee SJ, Vogelsang G, Flowers MED. Chronic graft-versus-host disease. *Biol Blood Marrow Transplant*. 2003;9:215–33.
- Atkinson K, Horowitz M, Gale R, Lee M, Rimm A, Bortin M. Consensus among bone marrow transplanters for diagnosis, grading and treatment of chronic graft-versus-host disease. Committee of the International Bone Marrow Transplant Registry. *Bone Marrow Transplant*. 1989;4:247–54.
- Filipovich AH, Weisdorf D, Pavletic S, et al. National Institutes of Health consensus development project on criteria for clinical trials in chronic graft-versus-host disease: I. Diagnosis and staging working group report. *Biol Blood Marrow Transplant*. 2005;11:945–56.
- Jagasia M, Giglia J, Chinratanalab W, et al. Incidence and outcome of chronic graft-versus-host disease using National Institutes of Health consensus criteria. *Biol Blood Marrow Transplant*. 2007;13:1207–15.
- Pérez-Simón J, Encinas C, Silva F, et al. Prognostic factors of chronic graft-versus-host disease following allogeneic peripheral blood stem cell transplantation: the National Institutes Health scale plus the type of onset can predict survival rates and the duration of immunosuppressive therapy. *Biol Blood Marrow Transplant*. 2008;14:1163–71.
- Cho B, Min C, Eom K, et al. Feasibility of NIH consensus criteria for chronic graft-versus-host disease. *Leukemia*. 2009;23:78–84.
- Arora M, Nagaraj S, Witte J, et al. New classification of chronic GVHD: added clarity from the consensus diagnoses. *Bone Marrow Transplant*. 2009;43:149–53.
- Kim D, Lee J, Kim S, et al. Reevaluation of the National Institutes of Health criteria for classification and scoring of chronic GVHD. *Bone Marrow Transplant*. 2010;45:1174–80.
- Flowers MED, Parker PM, Johnston LJ, et al. Comparison of chronic graft-versus-host disease after transplantation of peripheral blood stem cells versus bone marrow in allogeneic recipients: long-term follow-up of a randomized trial. *Blood*. 2002;100:415–9.
- Stewart B, Storer B, Storek J, et al. Duration of immunosuppressive treatment for chronic graft-versus-host disease. *Blood*. 2004;104:3501–6.
- Martin P, Weisdorf D, Przepiorka D, et al. National Institutes of Health Consensus Development Project on Criteria for clinical

- trials in chronic graft-versus-host disease: VI. Design of Clinical Trials Working Group report. *Biol Blood Marrow Transplant.* 2006;12:491–505.
27. Kitawaki T, Kadowaki N, Ishikawa T, Ichinohe T, Uchiyama T. Compromised recovery of natural interferon-alpha/beta-producing cells after allogeneic hematopoietic stem cell transplantation complicated by acute graft-versus-host disease and glucocorticoid administration. *Bone Marrow Transplant.* 2003;32:187–94.
 28. Mizumoto C, Kanda J, Ichinohe T, et al. Mycophenolate mofetil combined with tacrolimus and minidose methotrexate after unrelated donor bone marrow transplantation with reduced-intensity conditioning. *Int J Hematol.* 2009;89:538–45.
 29. Kanda J, Mizumoto C, Kawabata H, et al. Clinical significance of serum hepcidin levels on early infectious complications in allogeneic hematopoietic stem cell transplantation. *Biol Blood Marrow Transplant.* 2009;15:956–62.
 30. Przepiorka D, Weisdorf D, Martin P, et al. 1994 Consensus Conference on acute GVHD grading. *Bone Marrow Transplant.* 1995;15:825–8.
 31. Gooley TA, Leisenring W, Crowley J, Storer BE. Estimation of failure probabilities in the presence of competing risks: new representations of old estimators. *Stat Med.* 1999;18:695–706.
 32. Kim H. Cumulative incidence in competing risks data and competing risks regression analysis. *Clin Cancer Res.* 2007;13:559–65.
 33. Cortese G, Andersen P. Competing risks and time-dependent covariates. *Biom J.* 2010;52:138–58.
 34. Kim DH, Sohn SK, Baek JH, et al. Time to first flare-up episode of GVHD can stratify patients according to their prognosis during clinical course of progressive- or quiescent-type chronic GVHD. *Bone Marrow Transplant.* 2007;40:779–84.
 35. Flowers MED, Storer B, Carpenter P, et al. Treatment change as a predictor of outcome among patients with classic chronic graft-versus-host disease. *Biol Blood Marrow Transplant.* 2008;14:1380–4.
 36. Akpek G, Zahurak M, Piantadosi S, et al. Development of a prognostic model for grading chronic graft-versus-host disease. *Blood.* 2001;97:1219–26.
 37. Vigorito A, Campregher P, Storer B, et al. Evaluation of NIH consensus criteria for classification of late acute and chronic GVHD. *Blood.* 2009;114:702–8.

Separation of antileukemic effects from graft-versus-host disease in MHC-haploidentical murine bone marrow transplantation: participation of host immune cells

Atsushi Satake · Takayuki Inoue · Shuji Kubo · Yuki Taniguchi · Takehito Imado · Tatsuya Fujioka · Marika Horiuchi · Yunfeng Xu · Kazuhiro Ikegame · Satoshi Yoshihara · Katsuji Kaida · Hiroya Tamaki · Masaya Okada · Haruki Okamura · Hiroyasu Ogawa

Received: 12 November 2009 / Revised: 28 January 2010 / Accepted: 16 February 2010 / Published online: 20 March 2010
© The Japanese Society of Hematology 2010

Abstract Allogeneic hematopoietic stem cell transplantation (HSCT) is associated with both graft-versus-host disease (GVHD) and graft-versus-leukemia (GVL) effects. In clinical studies of HLA-mismatched HSCT, strong GVL effects have been reported. In the present study, we addressed the mechanism of the GVL and GVH response using MHC-haploidentical murine bone marrow transplantation (BMT) models. Recipient BDF1 (H-2^{b/d}) mice received T cell-depleted bone marrow and spleen cells from B6C3F1 (H-2^{b/k}) or C57BL/6 (H-2^b) mice with or without P815 mastocytoma cells (H-2^d) after receiving lethal total body irradiation. B6C3F1 → BDF1 (hetero-to-hetero type) recipients showed more powerful antileukemic effects with less severe GVHD than C57BL/6 → BDF1 (parent-to-F1 type) recipients. Compared with C57BL/6 → BDF1 recipients, significantly higher *in vitro* cytotoxic activity against P815 cells was observed in B6C3F1 → BDF1 recipients. Significantly lower CXCR3 expression on donor T cells and higher interferon (IFN)- γ expression were considered to be

associated with strong antileukemic effects with less severe GVHD in B6C3F1 → BDF1 recipients. Furthermore, host immune cells, especially natural killer cells and CD8⁺ T cells, were found to contribute remarkably to high IFN- γ production in B6C3F1 → BDF1 recipients. Thus, in MHC-haploidentical HSCT, host immune cells may change the balance between GVH and GVL response through IFN- γ production.

Keywords MHC-mismatched hematopoietic stem cell transplantation · GVHD · GVL · Interferon- γ · Natural killer cell

1 Introduction

Allogeneic hematopoietic stem cell transplantation (HSCT) has been a potentially curative therapy for patients with a variety of diseases, especially for hematologic malignancies [1, 2]; however, more than 70% of patients who could benefit from allogeneic bone marrow transplantation (BMT) do not have a matched sibling donor. On the other hand, there is a greater than 90% chance of promptly identifying a human leukocyte antigen (HLA)-haploidentical donor within the family. A major obstacle of HLA-mismatched HSCT is the high incidence of graft-versus-host disease (GVHD) [3, 4]; therefore, separating beneficial GVL effects from deleterious GVHD is a goal for HLA-mismatched HSCT.

In this context, we have reported, in a series of clinical studies on unmanipulated HLA-haploidentical HSCT, that strong graft-versus-leukemia (GVL) effects are maintained in many patients even after complete suppression of GVHD by the use of reduced-intensity conditioning treatment, or the use of steroids and/or anti-T-lymphocyte globulin as

A. Satake · T. Inoue · Y. Taniguchi · T. Imado · T. Fujioka · K. Ikegame · S. Yoshihara · K. Kaida · H. Tamaki · M. Okada · H. Ogawa (✉)
Division of Hematology, Department of Internal Medicine, Hyogo College of Medicine, 1-1 Mukogawa-cho, Nishinomiya, Hyogo 663-8501, Japan
e-mail: ogawah@hyo-med.ac.jp

S. Kubo · Y. Xu · H. Okamura
Laboratory of Host Defenses, Institute for Advanced Medical Sciences, Hyogo College of Medicine, Nishinomiya, Hyogo 663-8501, Japan

M. Horiuchi · H. Tamaki · H. Ogawa
Laboratory of Cell Transplantation, Institute for Advanced Medical Sciences, Hyogo College of Medicine, Nishinomiya, Hyogo 663-8501, Japan

GVHD prophylaxis [5–8]. However, the cellular and molecular mechanisms of the separation of GVL reaction from GVHD observed in HLA-haploidentical HSCT remain unclear. In murine BMT studies, parent-to-F1 (homo-to-hetero) BMTs, in which donor type engraftment can be achieved without total body irradiation (TBI), have usually been used as major histocompatibility complex (MHC)-haploidentical BMT models. Furthermore, these models have contributed to the progress of GVHD study [9] because the influence of radiation on tissue damage can be avoided; however, whether the parent-to-F1 murine models correctly reflect clinical HLA-haploidentical HSCTs that are mostly performed in transplant settings of HLA hetero-to-hetero combinations remains unclear.

To enable comparison between homo-to-hetero and hetero-to-hetero transplants, we therefore established two major MHC-haploidentical murine BMT models, in which recipient BDF1 (H-2^{b/d}) mice received T cell-depleted (TCD) bone marrow (BM) and spleen cells from B6C3F1 (H-2^{b/k}) or C57BL/6 (H-2^b) mice with or without P815 mastocytoma cells after receiving lethal TBI. In the present study, we found that B6C3F1 → BDF1 (MHC hetero-to-hetero-type) BMT showed more powerful antileukemic effects with less severe GVHD than C57BL/6 → BDF1 (MHC homo-to-hetero-type) BMT. Furthermore, we found that, compared with C57BL/6 → BDF1 recipients, B6C3F1 → BDF1 recipients showed lower CXCR3 expression on donor T cells in recipient spleens and higher interferon (IFN)- γ production. This high IFN- γ milieu with low expression of the inflammatory chemokine receptor was considered to be associated with the induction of strong antileukemic effects with less severe GVHD, since recent studies demonstrated that IFN- γ augmented lymphohematopoietic GVH reactions [10–12], namely, GVL reaction, and that IFN- γ mediated the protective effect against GVHD [13, 14]. Furthermore, donor immune cells as well as host immune cells, especially host natural killer (NK) cells and CD8⁺ T cells, were found to home to spleens after transplantation, and to produce IFN- γ highly in B6C3F1 → BDF1 recipients.

2 Materials and methods

2.1 Mice

Female C57BL/6 (B6, H-2^b), B6C3F1 (B6 × C3H/HeJ; H-2^{b/k}) or BDF1 (B6 × DBA2; H-2^{b/d}) mice were purchased from Japan CLEA (Osaka, Japan), or Shizuoka Laboratory Animal Center (Shizuoka, Japan). Mice used for experiments were 8–12 weeks of age, were housed in sterile microisolator cages in a specific pathogen-free mouse facility, and received autoclaved food and water ad libitum.

2.2 BMT

BM cells were harvested from the tibia and femur of donor mice by flushing with RPMI-1640 medium. T cell depletion of BM cells was performed by treatment with anti-Thy1.2 monoclonal antibody (mAb) (clone 30-H-12; PharMingen, San Diego, CA, USA) plus rabbit complement (Cedarlane, Hornby, ON, Canada). Spleen cells were isolated from donor mice using the nylon-wool-purification method as a source of lymphocytes. All BMTs were performed by the transfusion of a fixed number of donor cells after TBI the previous day. TBI was given in a single dose at a dose rate of 50 cGy/min. Cells from donors were resuspended in 0.5 ml RPMI-1640 medium and transplanted by tail-vein infusion into recipients.

Survival was monitored daily, and the presence of GVHD was judged by clinical symptoms, including body weight, posture (hunching), mobility, fur texture, and skin integrity [15]. All animal protocols were approved by the Ethics Review Committee for Animal Experimentation of Hyogo College of Medicine.

2.3 Challenge of tumor cells

In experiments to estimate the strength of antileukemic effects, recipient mice received P815 mastocytoma cells derived from DBA/2 (H-2^d). The tumor cells were injected intravenously through the tail vein on the day of transplantation.

2.4 Histopathological analysis

Tissues were fixed in 10% buffered formalin and embedded in paraffin. The sections were stained with hematoxylin and eosin and were examined by light microscopy. Immunohistochemical analysis was performed as previously described [16], with some modifications. In brief, frozen sections were fixed in 4% paraformaldehyde. After being blocked with phosphate-buffered saline (PBS) containing 10% fetal calf serum (FCS) for 15 min at room temperature, the origin of infiltrating T cells was determined by staining with mouse anti-H-2K^d mAb (SF1-1.1; host-specific) and rat anti-CD4 mAb (GK1.5) or rat anti-CD8 mAb (H35-17.2) at 4°C overnight and visualized using Alexa-Fluor 488-labeled anti-rat and Alexa-Fluor 546-labeled anti-mouse antibody. 4',6-Diamidino-2-phenylindole (DAPI) was used to stain the nucleus. Sections for fluorescent staining were analyzed with a confocal laser scanning microscope (LSM510; Carl Zeiss, Jena, Germany) [16].

2.5 In vivo spectral fluorescence imaging analysis

For in vivo imaging analysis, P815 cells were engineered to express mCherry fluorescent protein by a lentiviral vector

transduction system, as previously described [17, 18]. Recipient mice received modified P815 cells with BM and spleen cells via the tail vein on day 0. Prior to imaging, mice were anesthetized with sodium pentobarbital (Nembutal), and hair was removed with a hair removal cream, Epilat (Kracie, Tokyo, Japan), and rinsed with water. Spectral fluorescence imaging analysis was performed using the Maestro in vivo fluorescence imaging system (CRI; Woburn, MA, USA), as previously described [19]. Whole body images (0.05- to 0.5-s exposure) were taken and analyzed over sequential days.

2.6 Flow cytometric analysis

Anti-Fc receptor (2.4G2) monoclonal antibody (mAb), fluorescein isothiocyanate (FITC)-conjugated anti-mouse H-2K^d (clone SF1-1.1) mAb, phycoerythrin (PE)-indotricarbocyanine (Cy7)-conjugated anti-mouse CD3 (clone 145-2C11) mAb, anti-mouse CD4 (clone GK1.5) mAb, allophycocyanin (APC)-conjugated anti-mouse CD8 (clone 53-6.7) mAb, and PE-conjugated anti-mouse NK1.1 (clone PK136) mAb were purchased from PharMingen (San Diego, CA, USA). PE-conjugated anti-mouse CXCR3 (clone 220803) mAb and rat anti-mouse IgG_{2A} isotype control were purchased from R&D Systems (Minneapolis, MN, USA). Cell suspensions were prepared in PBS-containing 1% FCS and 0.1% sodium azide. Cells were incubated with an anti-Fc receptor mAb for 10 min at 4°C to block nonspecific staining and then incubated with FITC-, PE-Cy7-, APC-, and PE-conjugated mAb for 30 min. The stained cells were washed twice, resuspended, and analyzed using FACSCalibur (Becton–Dickinson, Mountain View, CA, USA) using CellQuest software (Becton–Dickinson).

Intracellular IFN- γ staining was performed using the BD Cytofix/CytopermTM Fixation/Permeabilization kit (BD Bioscience, San Jose, CA, USA). In brief, cells were retrieved from the recipient spleen, and resuspended at 10⁶/ml and cultured with phorbol myristic acid at 50 ng/ml plus ionomycin at 500 ng/ml for 5 h, including monensin during the last 2 h of culture. Cells were harvested, washed, and resuspended in PBS-containing 1% FCS and 0.1% sodium azide. Cell-surface antigens were then stained as described above, and cells were resuspended in 100 μ l per well of a microwell plate of fixation/permeabilization solution, and incubated for 20 min at 4°C. After washing, cells were stained with APC-conjugated anti-IFN- γ (clone XMG1.2; PharMingen) or isotype control: rat IgG1-APC (Clone R3-34).

2.7 Mixed lymphocyte culture (MLC) and ⁵¹Cr release assay

BDF1 mice were transplanted using TCD-BM (5×10^6) and spleen cells (2×10^7) after receiving TBI 9 Gy.

Spleen cells of the recipient mice on day 14 were used as responders for MLC. Cells ($3 \times 10^5/200 \mu$ l/well) were cultured with irradiated (20 Gy) BDF1 spleen cells ($3 \times 10^5/200 \mu$ l/well) in 24-well flat-bottomed plates (Falcon Labware, Lincoln Park, NJ, USA). After 72 h culture, IFN- γ concentrations of the culture supernatants were measured by Bio-Plex (Bio-Rad Laboratories, Hercules, CA, USA). For cytotoxic T lymphocyte (CTL) assay, BDF1 mice were transplanted using TCD-BM (5×10^6) and spleen cells (2×10^7) with P815 cells (1×10^4) after receiving TBI 9 Gy. Spleen cells of the recipient mice on day 14 were recovered, and directly measured for CTL activity against P815 cells by ⁵¹Cr release assay, as described elsewhere [20]. Effector cells were tested in triplicate at four effector:target (E:T) ratios, and the percent lysis was calculated according to the following formula: [(sample cpm – spontaneous cpm)/(maximum cpm – spontaneous cpm)] \times 100%. Results are shown as the mean percent lysis of the E:T cell ratio for each treatment group.

2.8 Statistical analysis

Values were compared by two-tailed Student's *t* test. Survival data were plotted by the Kaplan–Meier method and were analyzed by the log-rank test. A *P* value of less than 0.05 was considered significant.

3 Results

3.1 B6C3F1 \rightarrow BDF1 recipients showed less severe GVHD than C57BL/6 \rightarrow BDF1 recipients

To investigate the pathophysiology of GVH or GVL reactions in MHC-haploidentical BMT, we established 2 MHC-haploidentical murine BMT models: BDF1 (H-2^{b/d}) mice were transplanted from B6C3F1 (H-2^{b/k}) or C57BL/6 (H-2^b) mice. B6C3F1 \rightarrow BDF1 is an MHC hetero-to-hetero (donor/recipient combination) BMT model, where one MHC haplotype is identical between the donor and recipient but the other is different. C57BL/6 \rightarrow BDF1 is an MHC homo-to-hetero (parent-to-F1) BMT model, where MHC is haplotypically mismatched in the graft-versus-host (GVH) direction but not in the host-versus-graft (HVG) direction.

Recipient BDF1 mice received donor TCD-BM (5×10^6) and spleen (2×10^7) cells after a lethal TBI dose (9 Gy) the previous day. There was no significant difference in total cell numbers, T cell doses, and the CD4:CD8 ratio of spleen cells transfused between the 2 BMT models (data not shown). Two weeks after BMT, the majority of C57BL/6 \rightarrow BDF1 recipients began to present

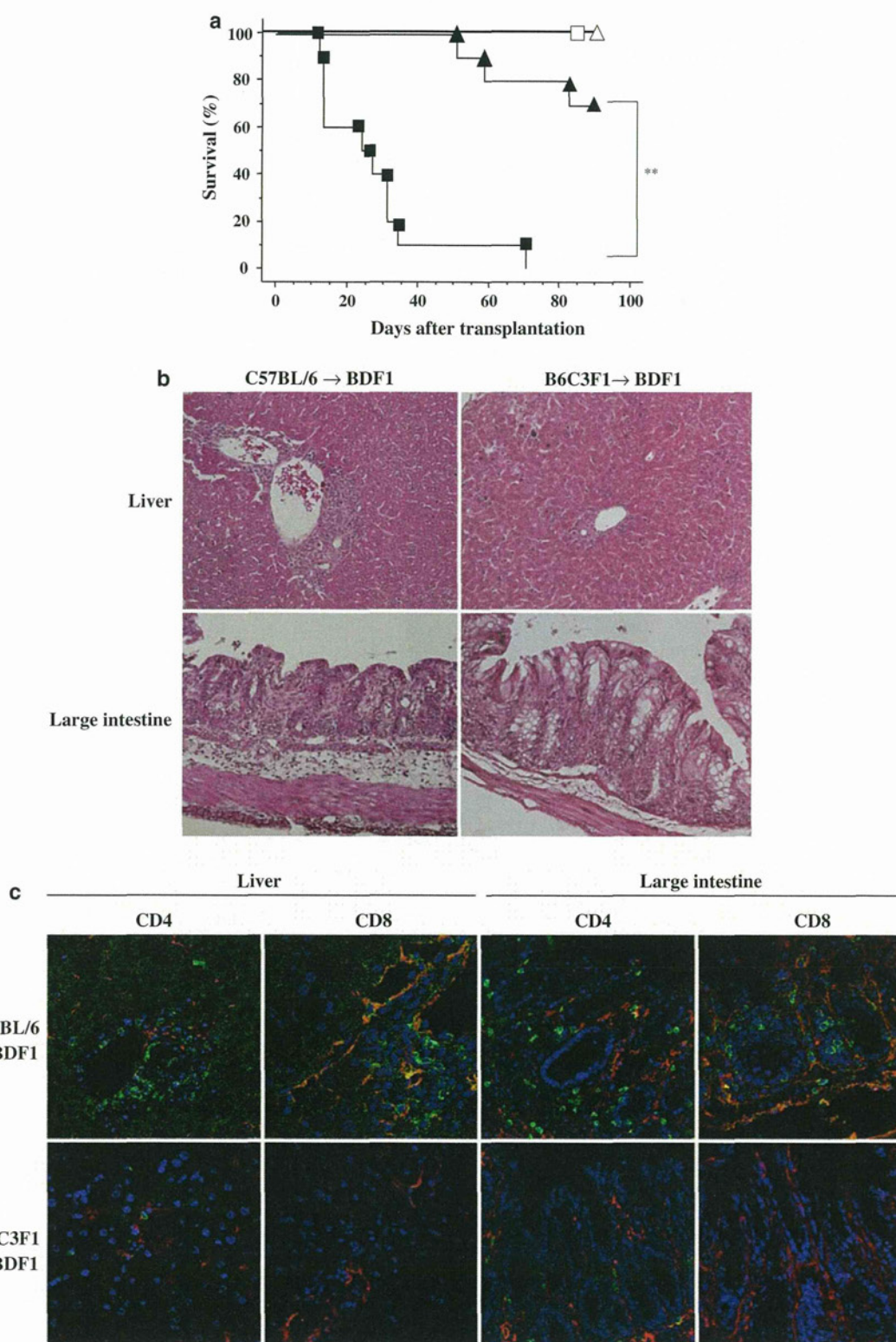
GVHD signs, such as body weight loss and a hunching posture, and 90% of mice had died of GVHD by day 40 (Fig. 1a). In contrast, B6C3F1 → BDF1 recipients showed fewer GVHD signs, and only 30% of mice had died of GVHD by day 80, with significantly improved survival observed in B6C3F1 → BDF1 recipients compared with C57BL/6 → BDF1 recipients. Histopathological examination of C57BL/6 → BDF1 recipients on day 14 revealed prominent lymphocyte infiltration in the periportal area of the liver, and various pathological changes in the large intestine compatible to GVHD (Fig. 1b, left panel). In the immunohistochemical study, these lymphocytes infiltrating the liver or large intestine were found to be donor-derived CD4 or CD8 T cells (Fig. 1c, upper panel). In contrast, liver or large intestine samples from B6C3F1 → BDF1 recipients showed few pathological changes (Fig. 1b, right panel) with almost no infiltration of donor T cells (Fig. 1c, lower panel). These results indicate that B6C3F1 → BDF1 recipients developed less severe GVHD than C57BL/6 → BDF1 recipients, leading to improved survival in B6C3F1 → BDF1 recipients.

3.2 B6C3F1 → BDF1 recipients induced more powerful antileukemic effects than C57BL/6 → BDF1 recipients

To compare antileukemic effects in the 2 MHC-haplo-identical BMTs, recipient BDF1 mice received P815 mastocytoma cells ($H-2^d$, 1×10^4) with donor TCD-BM cells (5×10^6) with or without donor spleen cells (2×10^7) after receiving TBI 9 Gy the previous day. In mice receiving TCD-BM cells alone, P815 cells proliferated mainly in the liver, spleen, and BM of the recipient, and tended to form macroscopic nodules in the liver or spleen. Some animals developed lower limb paralysis, and histological analysis revealed infiltration of P815 cells around the spinal cord. Thus, death of recipient mice accompanied by these signs or symptoms was considered leukemic death. When recipient mice presenting with clinical signs of GVHD died without any signs of leukemia progression, they were considered as death by GVHD. All mice receiving TCD-BM cells alone with P815 cells had died of leukemia progression by day 20 (Fig. 2a). Compared with mice receiving TCD-BM cells alone, mice receiving spleen cells showed a significantly improved survival in the 2 groups (Fig. 2a); however, none of them died of tumor progression (some mice died of GVHD). We could demonstrated antileukemic effects of donor spleen cells, but could not compare antileukemic effects in the 2 BMT models under these conditions.

Fig. 1 Survival and histological change in B6C3F1 → BDF1 and C57BL/6 → BDF1 recipients. **a.** Survival of B6C3F1 → BDF1 and C57BL/6 → BDF1 BMT recipients. All recipients receiving TCD-BM cells alone from C57BL/6 or B6C3F1 mice survived. For mice receiving TCD-BM and spleen cells, B6C3F1 → BDF1 mice showed significantly improved survival than C57BL/6 → BDF1 mice. All mice that died showed severe clinical signs of GVHD. *Open rectangles* C57BL/6 → BDF1 mice receiving TCD-BM cells only ($n = 4$); *open triangles* B6C3F1 → BDF1 mice receiving TCD-BM cells alone ($n = 4$), *closed rectangles* C57BL/6 → BDF1 mice receiving TCD-BM and spleen cells ($n = 10$), *closed triangles* B6C3F1 → BDF1 mice receiving TCD-BM and spleen cells ($n = 10$). ****P** value < 0.01. The results are representative of 2 separate experiments. **b** Histological analysis of the liver and large intestine from recipient mice receiving TCD-BM and spleen cells. Prominent lymphocyte infiltration in the periportal area of the liver and severe intestinal histopathological changes, including surface erosion, decreased numbers of goblet cells, and cellular infiltration in the lamina propria, were observed in samples from C57BL/6 → BDF1 recipients on day 14. In contrast, few pathological changes were observed in samples from B6C3F1 → BDF1 recipients. Representative data are shown ($\times 200$). **c** Immunohistochemical analysis of GVHD-target organs on day 12. Data represent multi-colored immunofluorescent staining: anti-CD4 (*green*) or anti-CD8 (*green*), anti-H2Kd (host-specific; *red*) and DAPI staining (*blue*) of the nucleus. Donor and host T cells were visualized as *green* and *yellow*, respectively. Massive lymphocytes infiltrating the liver or large intestine in C57BL/6 → BDF1 recipients were found to be donor-derived CD4 or CD8 T cells. In contrast, fewer infiltrates of donor T cells into these organs were observed in B6C3F1 → BDF1 recipients ($\times 300$)

Therefore, we decreased the number of spleen cells transfused to 5×10^5 cells. At this spleen cell dose, no mice died of GVHD. All mice receiving TCD-BM cells alone had died of tumor progression by day 14. Recipients receiving spleen cells survived significantly longer than mice receiving TCD-BM cells alone. All of C57BL/6 → BDF1 recipients receiving spleen cells had died of tumor progression by day 28, while only 20% of B6C3F1 → BDF1 recipients receiving spleen cells died of tumor progression during the observation period (Fig. 2b). For mice receiving spleen cells, compared with C57BL/6 → BDF1 recipients, B6C3F1 → BDF1 recipients showed a significant lower tumor mortality rate (Fig. 2b). To visualize the kinetics of tumor progression, P815 cells that were engineered to express mCherry fluorescent protein by a lentiviral transduction system were applied to the experiment in Fig. 2b. As shown in Fig. 2c, in mice receiving TCD-BM alone, fluorescence tumor signals appeared in the abdominal region (e.g. liver and spleen) and the femoral and sternal bones on day 10. In C57BL/6 → BDF1 recipients receiving TCD-BM and spleen cells, fluorescence tumor signals appeared in the femoral and sternal bones on day 10, and extended to the abdominal region by day 12. These fluorescence signals continued to strengthen, with signals continuing to spread



out to other organs, including the humeral bones and mesenteric lymph nodes, until death. Once mice became positive for fluorescence tumor signals, they always succumbed to

tumor. We killed some mice, and confirmed mCherry-positive P815 cells in the liver, spleen, and abdominal lymph nodes, as well as the bone marrow in the femoral, sternal,

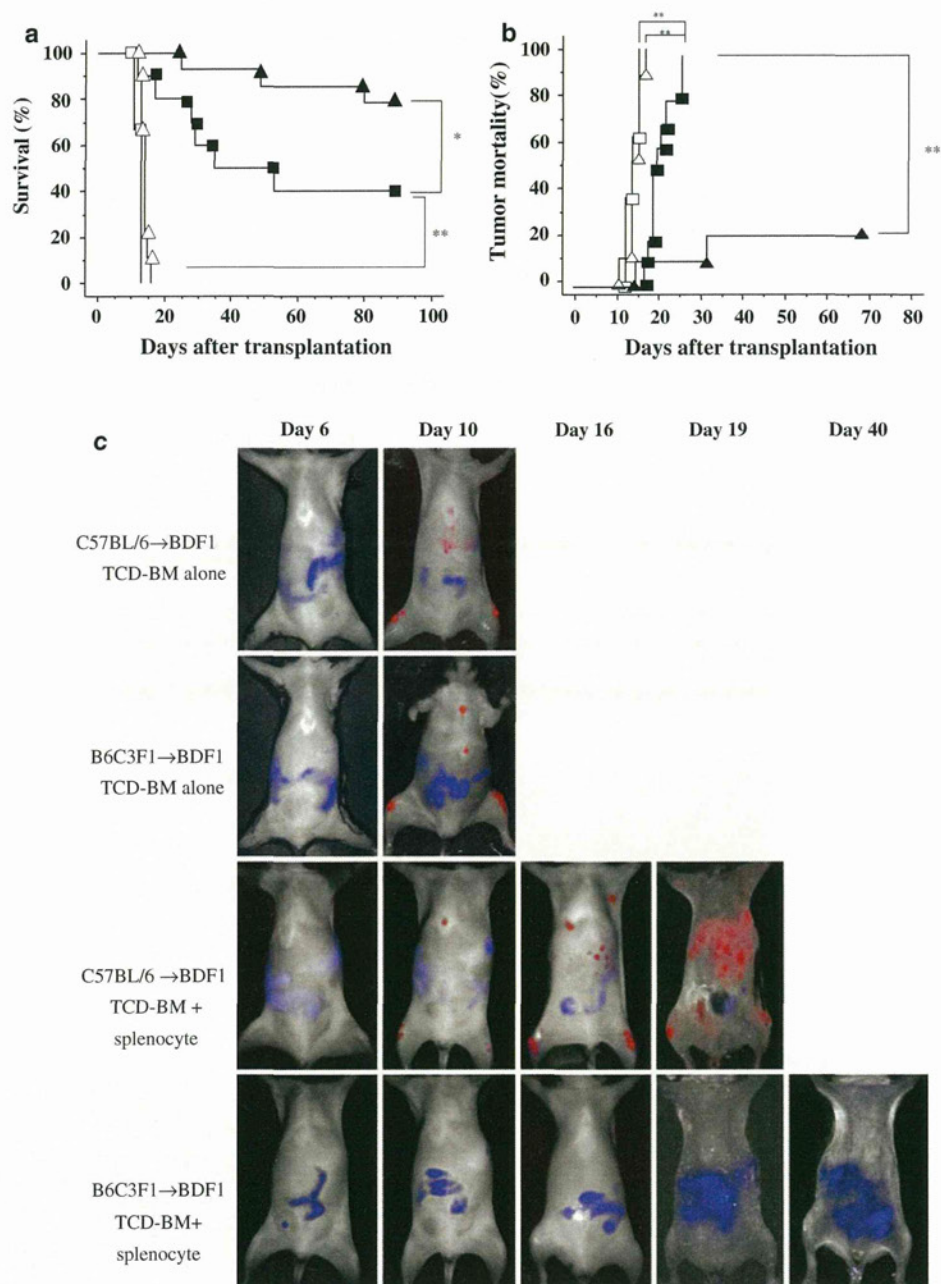


Fig. 2 B6C3F1 → BDF1 recipients developed stronger antileukemic effects than C57BL/6 → BDF1 recipients. **a** BDF1 mice received P815 mastocytoma cells ($H-2^d$, 1×10^4) with donor TCD-BM cells (5×10^6) with or without donor spleen cells (2×10^7) after receiving TBI 9 Gy the previous day. *Open rectangles* C57BL/6 → BDF1 mice receiving TCD-BM cells and P815 cells ($n = 6$), *open triangles* B6C3F1 → BDF1 receiving TCD-BM cells and P815 cells ($n = 9$), *closed rectangles* C57BL/6 → BDF1 mice receiving TCD-BM, spleen cells and P815 cells ($n = 10$), *closed triangles* B6C3F1 → BDF1 receiving TCD-BM, spleen cells and P815 cells ($n = 14$). * P value < 0.05 . Representative data from 3 separate experiments are shown. **b** The same experiments as in **a** were performed except for the reduced number of spleen cells transplanted

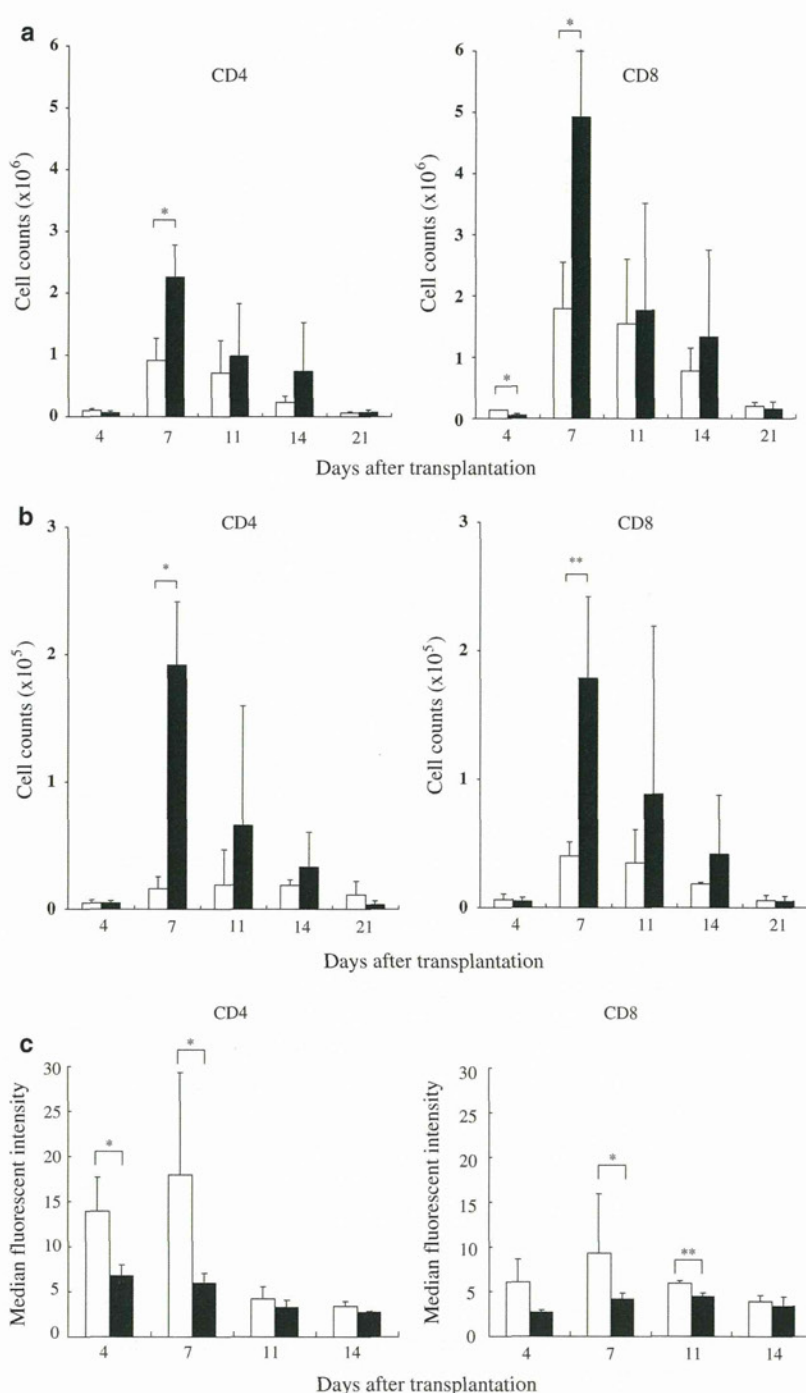
to 5×10^5 . Each *symbol* indicates the same mice as shown in **a**. ** P value < 0.01 . Representative data from 3 separate experiments are shown. **c** In vivo imaging analysis confirmed the difference in the kinetics of tumor progression between the 2 BMT groups. Transplantation was performed in the same condition as shown in **b**. P815 cells were engineered to express mCherry fluorescent protein by a lentiviral gene transduction system (see "Materials and methods"). Fluorescent imaging in mice was checked every other day from days 6 to 21, and thereafter once a week until day 40. Tumor mass of P815 cells and gastrointestinal contents are visualized as *red* and *blue*, respectively. Representative images from 2 independent experiments are shown

Fig. 3 The kinetics and characterization of T cells proliferating in recipient spleen.

a Kinetic analysis of donor T cells engrafted to recipient spleens. B6C3F1 → BDF1 and C57BL/6 → BDF1 BMTs were performed as shown in Fig. 1. The number of donor CD4⁺ or CD8⁺ T cells was calculated based on multi-colored flow cytometry data, as described in “Materials and methods”. *Open bars* C57BL/6 → BDF1 recipients, *closed bars* B6C3F1 → BDF1 recipients. Values were calculated based on experiments using at least 4 mice. Data are expressed as the mean ± standard deviation (SD). **P* < 0.05.

Representative data from 2 separate experiments are shown. **b** Kinetic analysis of host T cells recruited to recipient spleens. Each *symbol* indicates the same mice as shown in **a**. **P* < 0.05, ***P* < 0.01.

Representative data from 2 separate experiments are shown. **c** Median fluorescent intensity of CXCR3 expression on donor CD4⁺ and CD8⁺ T cells was compared in the 2 groups (*n* = 3). *Open bars* C57BL/6 → BDF1 recipients, *closed bars* B6C3F1 → BDF1 recipients. Results are representative of 2 experiments. **P* < 0.05, ***P* < 0.01



and humeral bones by fluorescence microscope and flow cytometry (data not shown). On the other hand, no detectable signals were observed in most B6C3F1 → BDF1 recipients receiving TCD-BM and spleen cells during the observation period. These results demonstrated that B6C3F1 → BDF1 recipients developed more powerful antileukemic effects despite presenting with less severe GVHD compared with C57BL/6 → BDF1 recipients.

3.3 Lower expression of CXCR3 on donor T cells engrafted to B6C3F1 → BDF1 spleens was associated with less severe GVHD

To address the difference in the extent of GVHD between B6C3F1 → BDF1 and C57BL/6 → BDF1 recipients (Fig. 1), we examined the kinetics of and characterized donor T cells engrafted to recipient spleens by flow

cytometry. As shown in Fig. 3a, CD8⁺ T cells dominated CD4⁺ T cells in the observation period, and donor T cells, being fewer on day 4, rapidly increased to peak on day 7, and thereafter decreased rapidly or gradually. On day 4, the number of CD8⁺ T cells in C57BL/6 → BDF1 recipients was significantly greater than in B6C3F1 → BDF1 recipients. On day 7, the number of CD4⁺ and CD8⁺ T cells in B6C3F1 → BDF1 recipients was significantly greater than that in C57BL/6 → BDF1 recipients. Regarding the kinetics of host T cells recruited to spleens, although 1 or 2 orders of magnitude lower than donor T cells, the number of host CD4⁺ and CD8⁺ T cells rapidly increased to peak on day 7, and thereafter decreased gradually (Fig. 3b). The numbers of CD4⁺ and CD8⁺ T cells on day 7 were significantly greater in B6C3F1 → BDF1 recipients than those in C57BL/6 → BDF1 recipients.

We next examined the CXCR3 expression status on donor T cells in recipient spleens. CXCR3 is a Th1-associated chemokine receptor, which plays an important role in the homing of donor T cells to GVHD-target organs [21, 22]. CXCR3 expression levels on donor T cells were highest on day 4, and thereafter decreased rapidly or gradually. Compared with B6C3F1 → BDF1 recipients, C57BL/6 → BDF1 recipients showed a significantly higher median fluorescent intensity of CXCR3 expression in CD4⁺ T cells on days 4 and 7, and in CD8⁺ T cells on days 7 and 11 (Fig. 3c). Regarding the expression of CCR5, another Th1-associated chemokine receptor, on donor T cells, the median fluorescent intensity of donor CD4⁺ or CD8⁺ T cells was also significantly higher in C57BL/6 → BDF1 recipients than in B6C3F1 → BDF1 recipients in the early transplantation days (data not shown). Thus, a relatively low CXCR3 or CCR5 expression on donor T cells proliferating in recipient spleen was considered to be associated with the occurrence of less severe GVHD in B6C3F1 → BDF1 recipients.

3.4 Stronger in vitro CTL activities and high IFN- γ expression in B6C3F1 → BDF1 recipients

To address the mechanism of stronger antileukemic activity in B6C3F1 → BDF1 recipients (Fig. 2), we next compared the production of inflammatory cytokines, TNF- α and IFN- γ , between B6C3F1 → BDF1 and C57BL/6 → BDF1 recipients. TNF- α is a well-known inflammatory cytokine to play a major role in inducing GVHD [23], while IFN- γ was recently reported to induce the separation of GVL effects from GVHD [11]. Serum TNF- α levels peaked on day 7, and thereafter decreased. There was no significant difference in serum TNF- α levels between the 2 groups (data not shown). On the other hand, serum IFN- γ levels were highest on day 4, and thereafter rapidly decreased (Fig. 4a). Serum IFN- γ levels on day 4 in

B6C3F1 → BDF1 recipients were significantly higher than in C57BL/6 → BDF1 recipients.

To ensure powerful antileukemic effects in B6C3F1 → BDF1 recipients, we performed an in vitro cytotoxicity assay against P815 cells. Using, as responders, spleen cells that were recovered from the recipient mice on day 14 in the experiment in Fig. 2a, we compared B6C3F1 → BDF1 and C57BL/6 → BDF1 BMTs. Responder cells used for cytotoxicity assay of C57BL/6 → BDF1 BMT were composed of a mean of 72.6% CD3⁺ cells (99.7% donor type; 18.0% CD4⁺ cells and 82.0% CD8⁺ cells) and a mean of 18.7% NK cells (88.2% donor type). Those of B6C3F1 → BDF1 BMT were composed of a mean of 71.2% CD3⁺ cells (100% donor type; 22.3% CD4⁺ cells and 77.7% CD8⁺ cells) and a mean of 9.7% NK cells (55.4% donor type). There was no significant difference in the percentage of CD4⁺ or CD8⁺ cells between C57BL/6 → BDF1 and B6C3F1 → BDF1 spleen cells. Recipient NK cell numbers in B6C3F1 → BDF1 spleen were significantly greater (around twice) than those in C57BL/6 → BDF1 spleen. As shown in Fig. 4b, spleen cells from B6C3F1 → BDF1 recipients showed significantly stronger CTL activities than those from C57BL/6 → BDF1 recipients. In addition, spleen cells recovered from recipients on day 14 were co-cultured with irradiated BDF1 spleen cells for 3 days, and we measured the IFN- γ concentration in the culture supernatant (Fig. 4c). Significantly higher IFN- γ production was observed in culture supernatants from B6C3F1 → BDF1 recipients than in those from C57BL/6 → BDF1 recipients. These results indicate that, compared with C57BL/6 → BDF1 recipients, B6C3F1 → BDF1 recipients have more powerful antileukemic effects, and also suggest that high IFN- γ production may have been involved in the induction of the powerful antileukemic effects.

3.5 Remarkable contribution of recipient immune cells to high IFN- γ production

To address the mechanism of high IFN- γ production in B6C3F1 → BDF1 recipients, we next intended to identify IFN- γ -secreting cells in recipient spleens. IFN- γ -secreting cells were calculated based on flow cytometry data using intracellular IFN- γ staining (Fig. 5a). In the analysis of whole mononuclear cells, on day 4, host-derived IFN- γ -secreting cells were significantly increased in B6C3F1 → BDF1 recipients than in C57BL/6 → BDF1 recipients but not donor-derived cells. On day 7, the number of IFN- γ -secreting cells in B6C3F1 → BDF1 recipients was significantly higher in both donor and host populations compared with in C57BL/6 → BDF1 recipients (Fig. 5b). In the analysis of each donor-derived lineage cell, there was no significant difference in the number

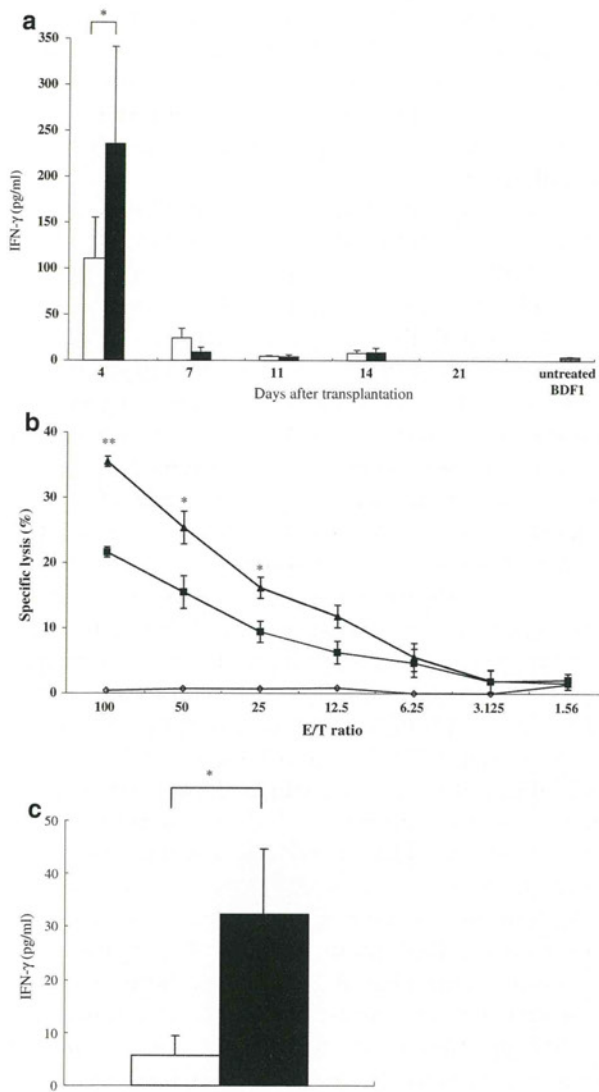


Fig. 4 Stronger in vitro CTL activity and higher IFN- γ expression in B6C3F1 \rightarrow BDF1 recipients. **a** Serum IFN- γ concentration in recipient mice. B6C3F1 \rightarrow BDF1 and C57BL/6 \rightarrow BDF1 BMTs were performed as shown in Fig. 1. Serum IFN- γ concentration was consecutively measured by Bio-Plex (see “Materials and methods”). Open bars C57BL/6 \rightarrow BDF1 recipients ($n = 8$), closed bars B6C3F1 \rightarrow BDF1 recipients ($n = 8$), gray bar untreated BDF1 mice ($n = 3$). Serum IFN- γ levels on day 21 became undetectable in the 2 BMT groups. Data are expressed as the mean \pm SD. * $P < 0.05$. Representative data from 2 separate experiments are shown. **b** In vitro cytotoxicity assay for P815 cells was performed using spleen cells on day 14. To obtain responders, mice received TCD-BM (5×10^6) and spleen (2×10^7) cells with P815 cells (1×10^4) after receiving TBI 9 Gy, as shown in Fig. 2a. Spleen cells were recovered from recipient mice on day 14, and directly checked for CTL activity against P815 cells by ^{51}Cr release assay, as described in “Materials and methods”. Closed triangles B6C3F1 \rightarrow BDF1 recipients, closed rectangles C57BL/6 \rightarrow BDF1 recipients, closed diamonds untreated BDF1 spleen cells. Values were calculated based on experiments using at least 4 samples. Data represent the mean \pm SD of specific lysis percentage for P815 cells at a given E/T ratio. Representative results from 2 independent experiments are shown. **c** IFN- γ production in the culture supernatants of mixed lymphocyte culture. B6C3F1 \rightarrow BDF1 and C57BL/6 \rightarrow BDF1 BMTs were performed as shown in Fig. 1. Spleen cells were recovered from recipient mice on day 14, and were co-cultured with irradiated (20 Gy) BDF1 spleen cells for 3 days, and the culture supernatant was checked for IFN- γ concentration by Bio-Plex (see “Materials and methods”). Open bar C57BL/6 \rightarrow BDF1 recipients, closed bar B6C3F1 \rightarrow BDF1 recipients. Values were calculated based on experiments using 5 samples. Data are expressed as the mean \pm SD. * $P < 0.05$. Representative results from 2 independent experiments are shown

4 Discussion

In the present study, using MHC-haploidentical murine BMT models, we showed that, compared with C57BL/6 \rightarrow BDF1 (homo-to-hetero-type BMT) recipients, B6C3F1 \rightarrow BDF1 (hetero-to-hetero-type BMT) recipients showed stronger antileukemic effects with less severe GVHD (Figs. 1, 2). Using these models, we addressed the mechanism by which B6C3F1 \rightarrow BDF1 BMT exerted stronger antileukemic effects with less severe GVHD than C57BL/6 \rightarrow BDF1 BMT, because clarification of the mechanism is considered to be useful for the understandings of the separation of GVL effects from GVHD in MHC-haploidentical HSCT.

Significantly higher antileukemic activity of B6C3F1 \rightarrow BDF1 recipients was also confirmed by in vitro cytotoxicity assay against P815 cells using spleen cells (Fig. 4b). We speculated that high IFN- γ production was involved in this higher antileukemic activity of B6C3F1 \rightarrow BDF1 recipients. In fact, serum IFN- γ levels in the early transplant period (on day 4) were significantly higher in B6C3F1 \rightarrow BDF1 recipients than in C57BL/6 \rightarrow BDF1 recipients (Fig. 4a), and IFN- γ levels in the culture supernatant for MLC were significantly higher than in C57BL/6 \rightarrow BDF1 recipients (Fig. 4c). We consider that this high IFN- γ production is not the effect but the cause of strong

of IFN- γ -secreting cells between the 2 BMT recipients except for CD8 $^+$ T cells on day 7 (Fig. 5c). When we calculated based on the donor T cell counts shown in Fig. 3a, the majority of CD8 $^+$ T cells in the 2 BMT recipients on day 4 were IFN- γ -secreting cells, with IFN- γ -secreting cells rapidly decreasing to only 10–15% on day 7. In the analysis of each host-derived lineage cell, IFN- γ -secreting cells were significantly increased in CD8 $^+$ T cells on day 7 and in NK cells on days 4 and 7 of B6C3F1 \rightarrow BDF1 recipients compared with C57BL/6 \rightarrow BDF1 recipients (Fig. 5d). In particular, the number of IFN- γ -secreting host NK cells on day 4 in B6C3F1 \rightarrow BDF1 recipients was 4 times higher than in C57BL/6 \rightarrow BDF1 recipients. These data strongly indicate that recipient immune cells, including T and NK cells, have highly contributed to high IFN- γ production in B6C3F1 \rightarrow BDF1 recipients.

allogeneic response. IFN- γ has been shown to enhance Th1 polarization through the facilitation of production of IL-12 by dendritic cells (DC) [24] or through synergizing with T cell receptor signals to maximally induce T-bet [25]. Furthermore, we demonstrated that host immune cells, especially NK cells, recruited to the spleen, substantially contributed to high IFN- γ production in B6C3F1 \rightarrow BDF1 recipients (Fig. 5). The fact that host NK cells still remained in recipient spleens on day 14 and the fact that the number of the host NK cells was significantly greater in B6C3F1 \rightarrow BDF1 spleens than in C57BL/6 \rightarrow BDF1 spleens support that host NK cells were more involved in high IFN- γ production in B6C3F1 \rightarrow BDF1 recipients. In particular, high IFN- γ production in spleen, a secondary lymphoid organ, is considered to be important for inducing strong antileukemic response. Although NK cells are largely excluded from lymph nodes under steady-state conditions, recruitment of NK cells to antigen-stimulated lymph nodes was recently reported to be important for providing an early source of IFN- γ that is necessary for Th1 polarization [26]. NK cells are also shown to participate in adaptive immune responses by modulating DC function or by producing IFN- γ [27].

Furthermore, IFN- γ has been reported to enhance GVL effects mainly by the following 2 mechanisms: the augmentation of lymphohematopoietic GVH reactions [10–12, 28] and enhancement of the susceptibility of tumor cells to alloresponses. Although the mechanism by which IFN- γ enhances lymphohematopoietic GVH reactions remains to be determined, this cytokine may mediate antihematopoietic activity that predominantly targets the recipient hematopoietic cells through its direct effect on hematopoietic cells [29]. IFN- γ may enhance the sensitivity of tumor cells to cytotoxic donor T cells by upregulating surface expressions of Fas and Fas-L, or MHC on tumor cells [30–32], or its direct effect on tumor cells [33].

The analysis of chemokine receptors [21, 22] on donor T cells engrafted to recipient spleens revealed that CD4⁺ or CD8⁺ T cells from B6C3F1 \rightarrow BDF1 recipients showed significantly lower CXCR3 expression levels, compared with those from C57BL/6 \rightarrow BDF1 recipients (Fig. 3c). These donor T cells in B6C3F1 \rightarrow BDF1 recipients, which also showed lower CCR5 expression (data not shown), were considered to have low ability to home to GVHD-target organs, which is a prerequisite for the induction of GVHD, despite highly expanding in the spleen. There was no significant difference in the serum levels of TNF- α , a major inducer of GVHD [23], between the 2 groups.

Regarding GVHD-protective effects of IFN- γ , IFN- γ inhibits T cell activation through various mechanisms, including the induction of apoptosis to alloreactive T cells [34], the inhibition of Th17 cells [35], the generation of

CD4 regulatory T cells [36], and the activation of immunosuppressive mesenchymal stem cells [37, 38], and furthermore the direct interaction of IFN- γ with recipient pulmonary parenchyma was recently reported to prevent idiopathic pneumonia syndrome in lethally irradiated mice after allogeneic HSCT [14].

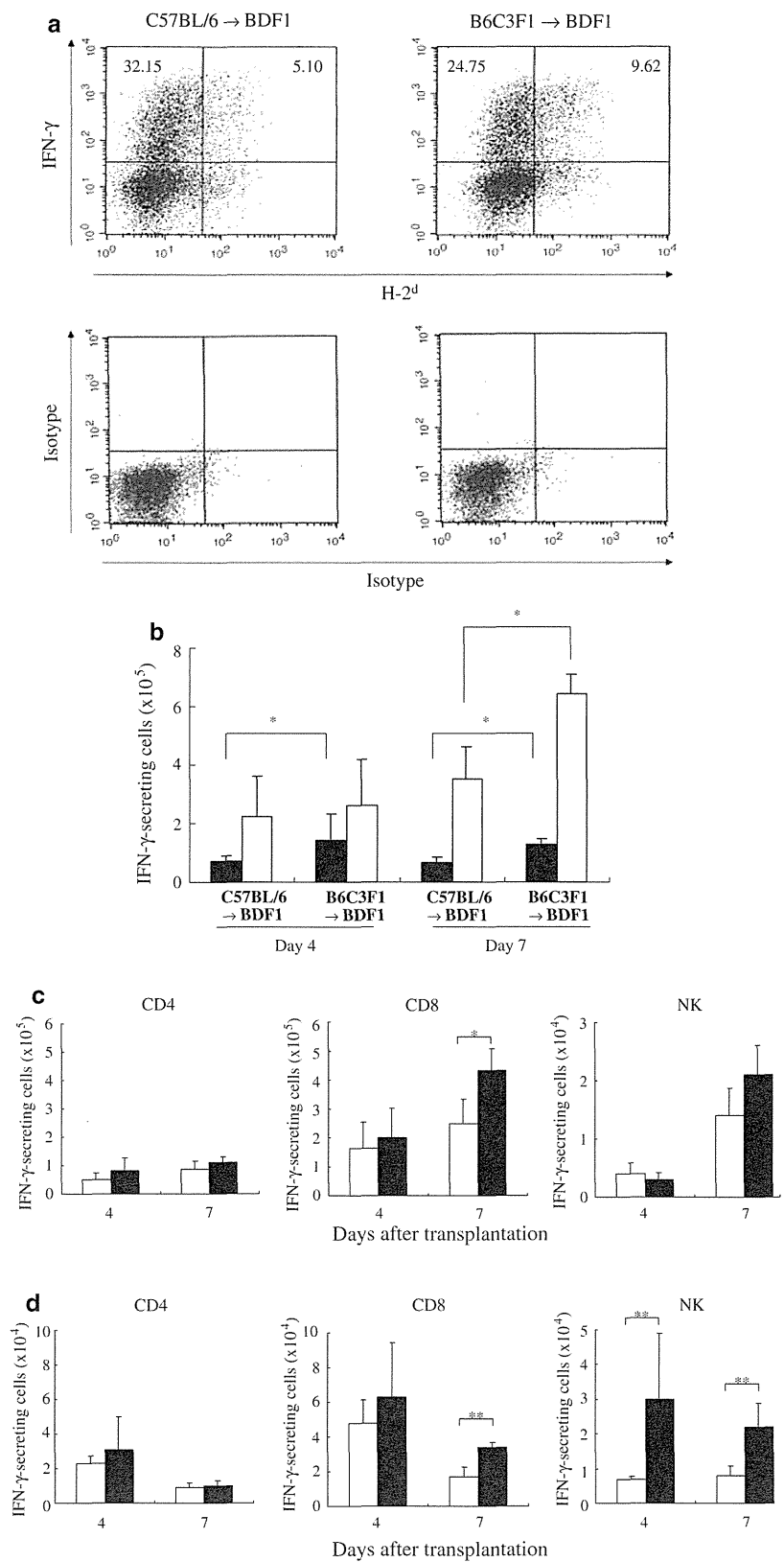
In the experiment using another MHC-haploidentical BMT models, C3D2F1 (H-2^{k/d}) \rightarrow B6C3F1 (H-2^{b/k}) and C3H (H-2^k) \rightarrow B6C3F1, stronger antileukemic effects for EL4 cells (H-2^b) with less severe GVHD were observed in C3D2F1 \rightarrow B6C3F1 recipients (hetero-to-hetero-type BMT) (data not shown). These findings suggest that separation of GVL effects from GVHD could be a generalized phenomenon observed mainly in hetero-to-hetero-type mismatched BMT; however, we need further experiments to confirm the hypothesis because the severity of GVHD is highly dependent on the strain combination in murine BMT models. Regarding the relationship between the findings in this animal study and our clinical data, we had 4 patients who underwent unmanipulated HLA-2-3 antigen-mismatched HSCT undergone in homo-to-hetero combination: 3 patients received myeloablative conditioning and the remaining 1 reduced-intensity conditioning. Two patients had no acute GVHD, 1 grade II GVHD, and the remaining early death. Among them, only 1 patient had a relapse. Homo-to-hetero combination does not seem to clinically develop severe GVHD, despite the experience of only 4 cases; however, the clinical outcome must have been influenced by intensive GVHD prophylaxis containing steroids in our HLA-haploidentical HSCT regimen [7, 8]. To obtain some clinical evidence, a large scale-study is needed, and we consider that the use of less intensified GVHD prophylaxis in our protocol may make the difference between homo-to-hetero and hetero-to-hetero combinations more evident in unmanipulated HLA-haploidentical transplant settings.

Our findings suggest that two-way in vivo MLC reaction occurs in spleens more strongly in hetero-to-hetero BMT recipients compared with homo-to-hetero BMT recipients, and that host immune cells, such as NK or T cells, produce IFN- γ abundantly, which may be considered to have contributed to the separation of GVL from GVHD. Thus, the participation of host hematopoietic cells in the afferent phase of GVHD changes the balance between allogeneic GVH and GVL responses of donor T lymphocytes, and that appropriate utilization of host immune cells may enable greater separation of GVL from GVH reactions.

In conclusion, we showed, in MHC-haploidentical murine BMT models, that powerful antileukemic effects with less severe GVHD were associated with a high production of IFN- γ , and also data suggesting that host immune cells, including NK cells, played an important role in this IFN- γ production.

Fig. 5 Contribution of recipient immune cells to high IFN- γ production in B6C3F1 \rightarrow BDF1 recipients. Transplantation was performed as shown in Fig. 1. IFN- γ -secreting cells in recipient spleens were calculated based on flow cytometry data using intracellular IFN- γ staining. * $P < 0.05$, ** $P < 0.01$.

a Representative flow cytometry data using whole mononuclear cells recovered from spleens on day 4. The *upper panels* indicate the percentages of IFN- γ -secreting cells in the fraction of whole mononuclear cells. *Dot plots* in which isotype-matched control mAb was used are shown in the *lower panels*. A higher percentage of host-derived (H-2^d positive) IFN- γ -secreting cells was observed in B6C3F1 \rightarrow BDF1 recipients than in C57BL/6 \rightarrow BDF1 recipients. **b** IFN- γ -secreting cells in the fraction of whole mononuclear cells retrieved from spleens on days 4 ($n = 7$) and 7 ($n = 4$). *Closed bars* host cells, *open bars* donor cells. **c** Donor-derived IFN- γ -secreting cells in each cell lineage. *Open bars* C57BL/6 \rightarrow BDF1 recipients, *closed bars* B6C3F1 \rightarrow BDF1 recipients. **d** Host-derived IFN- γ -secreting cells in each cell lineage. *Open bars* C57BL/6 \rightarrow BDF1 recipients, *closed bars* B6C3F1 \rightarrow BDF1 recipients. Regarding these IFN- γ -secreting cells, representative results from 2 independent experiments are shown



Acknowledgments We thank Kimiko Yamamoto, Hirotugu Kubo and Hatsuka Seki for technical assistance and also Dr. Tsuyoshi Iwasaki for helpful comments.

Conflict of interest statement The authors have no financial conflicts of interest.

References

1. Thomas ED. Karnofsky memorial lecture. Marrow transplantation for malignant diseases. *J Clin Oncol.* 1983;1:517–31.
2. Bortin MM, Rimm AA. Increasing utilization of bone marrow transplantation. *Transplantation.* 1986;42:229–34.
3. Gale RP. Graft-versus-host disease. *Immunol Rev.* 1985;88:193–214.
4. Ringden O, Nilsson B. Death by graft-versus-host disease associated with HLA mismatch, high recipient age, low marrow cell dose, and splenectomy. *Transplantation.* 1985;40:39–44.
5. Ikegami K, Tanji Y, Kitai N, Tamaki H, Kawakami M, Fujioka T, et al. Successful treatment of refractory T-cell acute lymphoblastic leukemia by unmanipulated stem cell transplantation from an HLA 3-loci mismatched (haploidentical) sibling. *Bone Marrow Transplant.* 2003;31:507–10.
6. Ogawa H, Ikegami K, Kawakami M, Tsuboi A, Kim EH, Hosen N, et al. Powerful graft-versus-leukemia effects exerted by HLA-haploidentical grafts engrafted with a reduced-intensity regimen for relapse following myeloablative HLA-matched transplantation. *Transplantation.* 2004;78:488–9.
7. Ogawa H, Ikegami K, Yoshihara S, Kawakami M, Fujioka T, Masuda T, et al. Unmanipulated HLA 2–3 antigen-mismatched (haploidentical) stem cell transplantation using nonmyeloablative conditioning. *Biol Blood Marrow Transplant.* 2006;12:1073–84.
8. Ogawa H, Ikegami K, Kaida K, Yoshihara S, Fujioka T, Tanguchi Y, et al. Unmanipulated HLA 2–3 antigen-mismatched (haploidentical) bone marrow transplantation using only pharmacological GVHD prophylaxis. *Exp Hematol.* 2008;36:1–8.
9. Murai M, Yoneyama H, Ezaki T, Suematsu M, Terashima Y, Harada A, et al. Peyer's patch is the essential site in initiating murine acute and lethal graft-versus-host reaction. *Nat Immunol.* 2003;4:154–60.
10. Welniak LA, Blazar BR, Anver MR, Wiltout RH, Murphy WJ. Opposing roles of interferon-gamma on CD4+ T cell-mediated graft-versus-host disease: effects of conditioning. *Biol Blood Marrow Transplant.* 2000;6:604–12.
11. Yang YG, Qi J, Wang MG, Sykes M. Donor-derived interferon gamma separates graft-versus-leukemia effects and graft-versus-host disease induced by donor CD8 T cells. *Blood.* 2002;99:4207–15.
12. Wang H, Asavaroengchai W, Yeap BY, Wang MG, Wang S, Sykes M, et al. Paradoxical effects of IFN-gamma in graft-versus-host disease reflect promotion of lymphohematopoietic graft-versus-host reactions and inhibition of epithelial tissue injury. *Blood.* 2009;113:3612–9.
13. Brok HP, Heidt PJ, van der Meide PH, Zurcher C, Vossen JM. Interferon-gamma prevents graft-versus-host disease after allogeneic bone marrow transplantation in mice. *J Immunol.* 1993;151:6451–9.
14. Burman AC, Banovic T, Kuns RD, Clouston AD, Stanley AC, Morris ES, et al. IFN γ differentially controls the development of idiopathic pneumonia syndrome and GVHD of the gastrointestinal tract. *Blood.* 2007;110:1064–72.
15. Cooke KR, Kobzik L, Martin TR, Brewer J, Delmonte J Jr, Crawford JM, et al. An experimental model of idiopathic pneumonia syndrome after bone marrow transplantation. I. The roles of minor H antigens and endotoxin. *Blood.* 1996;88:3230–9.
16. Yoshida Y, Hirano T, Son G, Iimuro Y, Imado T, Iwasaki T, et al. Allogeneic bone marrow transplantation for hepatocellular carcinoma: hepatocyte growth factor suppresses graft-vs.-host disease. *Am J Physiol Gastrointest Liver Physiol.* 2007;293:G1114–23.
17. Kubo S, Seleme MC, Soifer HS, Perez JL, Moran JV, Kazanian HH Jr, et al. L1 retrotransposition in nondividing and primary human somatic cells. *Proc Natl Acad Sci USA.* 2006;103:8036–41.
18. Nakagomi N, Nakagomi T, Kubo S, Nakano-Doi A, Saino O, Takata M, et al. Endothelial cells support survival, proliferation and neuronal differentiation of transplanted adult ischemia-induced neural stem/progenitor cells after cerebral infarction. *Stem Cells.* 2009;27:2185–95.
19. Barrett T, Koyama Y, Hama Y, Ravizzini G, Shin IS, Jang BS, et al. In vivo diagnosis of epidermal growth factor receptor expression using molecular imaging with a cocktail of optically labeled monoclonal antibodies. *Clin Cancer Res.* 2007;13:6639–48.
20. Iwasaki T, Fujiwara H, Shearer GM. Loss of proliferative capacity and T cell immune development potential by bone marrow from mice undergoing a graft-vs-host reaction. *J Immunol.* 1986;137:3100–8.
21. Jaksch M, Remberger M, Mattsson J. Increased gene expression of chemokine receptors is correlated with acute graft-versus-host disease after allogeneic stem cell transplantation. *Biol Blood Marrow Transplant.* 2005;11:280–7.
22. Sackstein R. A revision of Billingham's tenets: the central role of lymphocyte migration in acute graft-versus-host disease. *Biol Blood Marrow Transplant.* 2006;12:2–8.
23. Hill GR, Ferrara JL. The primacy of the gastrointestinal tract as a target organ of acute graft-versus-host disease: rationale for the use of cytokine shields in allogeneic bone marrow transplantation. *Blood.* 2000;95:2754–9.
24. Snijders A, Kalinski P, Hilkens CM, Kapsenberg ML. High-level IL-12 production by human dendritic cells requires two signals. *Int Immunol.* 1998;10:1593–8.
25. Afkarian M, Sedy JR, Yang J, Jacobson NG, Cereb N, Yang SY, et al. T-bet is a STAT1-induced regulator of IL-12R expression in naive CD4+ T cells. *Nat Immunol.* 2002;3:549–57.
26. Martín-Fontecha A, Thomsen LL, Brett S, Gerard C, Lipp M, Lanzavecchia A, et al. Induced recruitment of NK cells to lymph nodes provides IFN- γ for TH1 priming. *Nat Immunol.* 2004;5:1260–5.
27. Moretta A. Natural killer cells and dendritic cells: rendezvous in abused tissues. *Nat Rev Immunol.* 2002;2:957–64.
28. Pelot MR, Pearson DA, Swenson K, Zhao G, Sachs J, Yang YG, et al. Lymphohematopoietic graft-vs.-host reactions can be induced without graft-vs.-host disease in murine mixed chimeras established with a cyclophosphamide-based nonmyeloablative conditioning regimen. *Biol Blood Marrow Transplant.* 1999;5:133–43.
29. Rottman M, Soudais C, Vogt G, Renia L, Emile JF, Decaluwe H, et al. IFN-gamma mediates the rejection of hematopoietic stem cells in IFN-gammaR1-deficient hosts. *PLoS Med.* 2008;5:e26.
30. Böhm W, Thoma S, Leithäuser F, Möller P, Schirmbeck R, Reimann J. T cell-mediated, IFN-gamma-facilitated rejection of murine B16 melanomas. *J Immunol.* 1998;161:897–908.
31. Sayers TJ, Brooks AD, Lee JK, Fenton RG, Komschlies KL, Wigginton JM, et al. Molecular mechanisms of immune-mediated lysis of murine renal cancer: differential contributions of perforin-dependent versus Fas-mediated pathways in lysis by NK and T cells. *J Immunol.* 1998;161:3957–65.
32. Puliaev R, Nguyen P, Finkelman FD, Via CS. Differential requirement for IFN-gamma in CTL maturation in acute murine graft-versus-host disease. *J Immunol.* 2004;173:910–9.

33. Sayers TJ, Wiltout TA, McCormick K, Husted C, Wiltout RH. Antitumor effects of alpha-interferon and gamma-interferon on a murine renal cancer (Renca) in vitro and in vivo. *Cancer Res.* 1990;50:5414–20.
34. Badovinac VP, Tvinnereim AR, Harty JT. Regulation of antigen-specific CD8+ T cell homeostasis by perforin and interferon-gamma. *Science.* 2000;17:1354–8.
35. Harrington LE, Hatton RD, Mangan PR, Turner H, Murphy TL, Murphy KM, et al. Interleukin 17-producing CD4+ effector T cells develop via a lineage distinct from the T helper type 1 and 2 lineages. *Nat Immunol.* 2005;6:1123–32.
36. Sawitzki B, Kingsley CI, Oliveira V, Karim M, Herber M, Wood KJ. IFN-gamma production by alloantigen-reactive regulatory T cells is important for their regulatory function in vivo. *J Exp Med.* 2005;201:1925–35.
37. Polchert D, Sobinsky J, Douglas GW, Kidd M, Moadsiri A, Reina E, et al. IFN- γ activation of mesenchymal stem cells for treatment and prevention of graft versus host disease. *Eur J Immunol.* 2008;38:1745–55.
38. English K, Barry FP, Field-Corbett CP, Mahon BP. IFN-gamma and TNF-alpha differentially regulate immunomodulation by murine mesenchymal stem cells. *Immunol Lett.* 2007;110:91–100.

Reproduced with permission of the copyright owner. Further reproduction prohibited without permission.

Hepatosplenic $\alpha\beta$ T cell lymphoma

Yuya Nagai · Kazuhiro Ikegame · Minako Mori · Daichi Inoue · Takaharu Kimura · Sonoko Shimoji · Katsuhiko Togami · Sumie Tabata · Masayuki Kurata · Yukihiro Imai · Akiko Matsushita · Kenichi Nagai · Hiroyasu Ogawa · Takayuki Takahashi

Received: 28 April 2009 / Accepted: 28 August 2009 / Published online: 10 March 2010
© Japan Society of Clinical Oncology 2010

Abstract A 32-year-old male with chronic hepatitis B was admitted to a hospital with cellulitis in the right leg in September 2006. Pancytopenia, hepatosplenomegaly, and systemic superficial lymph node swelling were noted, and he was referred to our hospital. He developed fever and liver dysfunction in June 2007 and underwent a splenectomy. His pancytopenia subsequently improved. A pathologic diagnosis of hepatosplenic $\alpha\beta$ T cell lymphoma was made by examining spleen tissue and biopsy specimens of the liver and mesenteric lymph node. He had stage IVB disease because neoplastic T cells were noted in the bone marrow. The response of the lymphoma to conventional chemotherapy including the CHOP (cyclophosphamide, adriamycin, vincristine, prednisolone) and DeVIC (dexamethasone, etoposide, ifoshamide, carboplatin) regimens was poor and transient. A partial remission was obtained with an ESHAP (etoposide, cisplatin, cytarabine, methylprednisolone) regimen. Therefore, we planned a bone marrow transplantation (BMT) from an HLA-haploidentical sibling donor. He was moved to the Department of

Hematology, Hyogo Medical College, to receive this BMT as part of a clinical trial. During the conditioning procedure for the transplantation, however, he died of septicemia. Since hepatosplenic $\alpha\beta$ T cell lymphoma is very rare with only 23 reported cases to date, herein we report this case and discuss the therapeutic strategy.

Keywords Hepatosplenic T cell lymphoma · Alpha-beta T cell · Allogeneic hematopoietic stem cell transplantation

Introduction

Hepatosplenic lymphoma of $\gamma\delta$ T cell origin is a rare subtype of peripheral T cell lymphoma, which was first reported by Farcet et al. [1]. Another hepatosplenic T cell lymphoma (HSTCL) with the $\alpha\beta$ type T cell receptor (TCR) was reported in 2000 [2, 3]. This subtype is even rarer, with only 23 cases reported to date [1–3, 5, 7–11]. At present, both subtypes of HSTCL are recognized as a distinct entity of malignant lymphoma in the WHO classification system [4]. $\alpha\beta$ HSTCL exhibits an aggressive clinical course with a poor prognosis. Indeed, almost all patients who received conventional chemotherapy for lymphoma died of disease progression [5]. Therefore, hematopoietic stem cell transplantation (HSCT) has been conducted as a curative therapeutic modality [3, 7–11]. In a case report of $\gamma\delta$ HSTCL associated with chronic hepatitis B, Ozaki et al. [6] discussed the possible role of the HBV infection in the pathogenesis; however, for the $\alpha\beta$ type, there has been neither a reported case of $\alpha\beta$ HSTCL associated with chronic HBV infection nor study regarding the role of HBV in the pathogenesis of this type of HSTL.

Y. Nagai · M. Mori · D. Inoue · T. Kimura · S. Shimoji · K. Togami · S. Tabata · M. Kurata · A. Matsushita · K. Nagai · T. Takahashi (✉)
Department of Hematology and Clinical Immunology,
Kobe City Medical Center General Hospital,
4-6 Minatojima-Nakamachi, Chuo-ku,
Kobe 650-0046, Japan
e-mail: sonata53@kcgh.gr.jp

Y. Imai
Department of Clinical Pathology,
Kobe City Medical Center General Hospital, Kobe, Japan

K. Ikegame · H. Ogawa
Division of Hematology, Department of Internal Medicine,
Hyogo Medical College, Hyogo, Japan

Case report

A 32-year-old male with chronic hepatitis B was admitted to a hospital with cellulites secondary to atopic dermatitis in the right leg in September 2006. He had hepatosplenomegaly and superficial lymphadenopathy and was pancytopenic. Based on the examination of biopsy specimens of inguinal and cervical lymph nodes, he was pathologically diagnosed with reactive lymphadenitis. He was referred to our hospital because of pancytopenia in May 2007. Physical examination showed hepatomegaly (6 cm below the costal margin), splenomegaly (10 cm below the costal margin), and systemic superficial lymphadenopathy with a diameter of around 1.5 cm. A bone marrow aspirate did not show any dysplastic features of hematopoietic cells. He was admitted to our hospital because of B symptoms (fever, weight loss, and night sweating) and liver dysfunction in June 2007. Hematologic examination showed a white blood cell count of $7 \times 10^9/l$ with a normal differential count, a platelet count of $33 \times 10^9/l$, and a hemoglobin concentration of 10.7 g/dl. Hemostatic examination revealed a fibrinogen concentration of 75 mg/dl (normally 180–320), D-dimer concentration of 8.7 $\mu\text{g/ml}$ (normally below 1.0), thrombin-antithrombin complex (TAT) concentration of 37.4 ng/ml (normally below 3.2), and $\alpha 2$ -plasmin inhibitor complex (PIC) concentration of 4.5 $\mu\text{g/ml}$ (normally below 0.799), indicating disseminated intravascular coagulation (DIC). Biochemical tests revealed

AST concentration of 319 IU/l, ALT concentration of 292 IU/l, LDH concentration of 1,011 IU/l (120–250), total bilirubin concentration of 1.1 mg/dl, ALP concentration of 451 IU/l (100–340), and γ GTP concentration of 41 IU/l. Concentrations of C-reactive protein (CRP) and soluble interleukin-2 receptor (sIL-2R) were elevated to 1.5 mg/dl (normally below 0.5) and 11,100 U/ml (below 530), respectively. Serological tests for hepatitis B (HBs-Ag and HBe-Ab) gave positive results. The loading of hepatitis B virus (HBV-DNA) was 3.2 log copy/ml (normally below 2.6). Neither anti-human T-cell lymphotropic virus type 1 (HTLV-1) nor anti human immunodeficiency virus (HIV) antibodies were detected. Positron emission tomography-computed tomography (PET-CT) scanning with FDG showed hepatomegaly, a huge spleen that almost occupied the entire pelvic cavity, and lymph node swelling in the abdominal cavity (Fig. 1). We conducted splenectomy and the biopsy of liver tissue and lymph nodes to make a definite diagnosis and to improve the thrombocytopenia after splenectomy. The weight of the spleen was 5 kg. The splenic capsule was intact, and the cut surface was homogeneously red-purple without nodulation. Microscopically, massive infiltration of medium-sized lymphocytes in the red pulp was observed, and these cells had cleaved nuclei and scant to moderate cytoplasm. In the liver, similar lymphocytes markedly and moderately infiltrated the sinusoids and periportal region, respectively. In the lymph node, the normal architecture was completely effaced by the same abnormal

Fig. 1 CT and positron emission tomography (PET)-CT scanning. **a** CT scans showing hepatomegaly and marked splenomegaly. **b** An abnormal accumulation of FDG in the spleen and superficial lymph nodes and in the abdominal cavity is seen

